ANL-7695
RETURN TO ANL (IDAHO) LIBRARY.

ANL-7695

Argonne National Laboratory

EXPERIMENTAL RESULTS FOR ZPR-3 ASSEMBLIES 58 AND 59

by

J. M. Stevenson, J. M. Gasidlo,
V. C. Rogers, G. G. Simons,
and R. O. Vosburgh

The facilities of Argonne National Laboratory are owned by the United States Government. Under the terms of a contract (W-31-109-Eng-38) between the U. S. Atomic Energy Commission, Argonne Universities Association and The University of Chicago, the University employs the staff and operates the Laboratory in accordance with policies and programs formulated, approved and reviewed by the Association.

MEMBERS OF ARGONNE UNIVERSITIES ASSOCIATION

The University of Arizona
Carnegie-Mellon University
Case Western Reserve University
The University of Chicago
University of Cincinnati
Illinois Institute of Technology
University of Illinois
Indiana University
Iowa State University
The University of Iowa
Kansas State University
The University of Kansas
Loyola University
Marquette University
Michigan State University
The University of Michigan
University of Minnesota
University of Missouri
Northwestern University
University of Notre Dame
The Ohio State University
Ohio University
The Pennsylvania State University
Purdue University
Saint Louis University
Southern Illinois University
The University of Texas at Austin
Washington University
Wayne State University
The University of Wisconsin

NOTICE

This report was prepared as an account of work sponsored by the United States Government. Neither the United States nor the United States Atomic Energy Commission, nor any of their employees, nor any of their contractors, subcontractors, or their employees, makes any warranty, express or implied, or assumes any legal liability or responsibility for the accuracy, completeness or usefulness of any information, apparatus, product or process disclosed, or represents that its use would not infringe privately-owned rights.

Printed in the United States of America
Available from
National Technical Information Service
U.S. Department of Commerce
Springfield, Virginia 22151
Price: Printed Copy $3.00; Microfiche $0.65

ANL-7695
Reactor Technology

ARGONNE NATIONAL LABORATORY
9700 South Cass Avenue
Argonne, Illinois 60439

EXPERIMENTAL RESULTS FOR ZPR-3 ASSEMBLIES 58 AND 59

by

J. M. Stevenson, J. M. Gasidlo,
V. C. Rogers, G. G. Simons,
and R. O. Vosburgh

Applied Physics Division

April 1970

TABLE OF CONTENTS

	Page
ABSTRACT	7
I. INTRODUCTION	7
II. SELECTION OF ASSEMBLIES 58 AND 59	7
III. ASSEMBLY COMPOSITIONS AND CRITICAL MASSES	9
IV. CALIBRATION OF SAFETY RODS, CONTROL RODS, AND AUTORODS	12
V. FISSION-RATE DISTRIBUTIONS	14
VI. PERTURBATION DISTRIBUTIONS	19
VII. CENTRAL FISSION RATIOS	24
VIII. CENTRAL PERTURBATIONS	24
IX. CENTRAL SUBSTITUTION MEASUREMENTS	26
X. DOPPLER REACTIVITY EFFECT OF NATURAL URANIUM OXIDE	28
XI. CENTRAL NEUTRON SPECTRUM USING PROTON-RECOIL COUNTERS	29
APPENDIX--Safety Analysis of Assemblies 58 and 59	37
ACKNOWLEDGMENTS	39
REFERENCES	40

LIST OF FIGURES

No.	Title	Page
1.	Core Drawer Loading for Assembly 58	9
2.	Reference Core Loading for Assembly 58	10
3.	Reference Core Loading for Assembly 59	10
4.	Equivalent Cylindrical Dimensions for Assembly 58	12
5.	Axial Traverse Drawer Loading in Half 1 of Assembly 59	15
6.	^{239}Pu Fission-rate Radial Traverse in Assembly 58	16
7.	^{238}U Fission-rate Radial Traverse in Assembly 58	17
8.	^{239}Pu Fission-rate Radial Traverse in Assembly 59	17
9.	^{238}U Fission-rate Radial Traverse in Assembly 59	18
10.	^{239}Pu Fission-rate Axial Traverse in Assembly 59	18
11.	^{238}U Fission-rate Axial Traverse in Assembly 59	18
12.	^{239}Pu Perturbation Radial Traverse in Assembly 58	20
13.	^{238}U Perturbation Radial Traverse in Assembly 58	21
14.	^{239}Pu Perturbation Radial Traverse in Assembly 59	21
15.	^{239}Pu Perturbation Axial Traverse in Assembly 59	22
16.	^{252}Cf Source-perturbation Radial Traverse in Assembly 59	23
17.	^{252}Cf Source-perturbation Axial Traverse in Assembly 59	23
18.	Core Drawer for Back-to-Back Fission Counter	24
19.	Half-inch Voided Drawer for Central Perturbations	25
20.	Core Drawer for Doppler Sample in Assembly 59	28
21.	0.625-in.-diam Hydrogen Proportional Counter and Preamplifier Installed in Special Drawer	29
22.	Neutron Spectrum from Proton-recoil Proportional Counters	35

LIST OF TABLES

No.	Title	Page
I.	Composition of Assembly 58	11
II.	Average Core and Reflector Compositions of Assembly 59	11
III.	Delayed-neutron Data for Control-rod Calibrations	12
IV.	Group Decay Constants for Delayed Neutrons	13
V.	Worths of Control and Safety Rods	13
VI.	Traverse Counter Specifications	14
VII.	Fission-rate Radial Traverses in Assembly 58	15
VIII.	Fission-rate Radial Traverses in Assembly 59	16
IX.	Fission-rate Axial Traverses in Assembly 59	16
X.	Perturbation Radial Traverses in Assembly 58	19
XI.	Plutonium-239 Perturbation Traverses in Assembly 59	20
XII.	Californium-252 Source Perturbation Traverses in Assembly 59	23
XIII.	Central Fission Ratios in Assembly 59	24
XIV.	Central Perturbation Results	25
XV.	Ratios of Central Perturbations	26
XVI.	Reactivity Worth of Central Substitution Experiments in Assembly 59	27
XVII.	Reactivity Changes of Natural UO_2 Sample	29
XVIII.	Neutron Spectrum from Proton-recoil Proportional Counters	31
XIX.	Neutron Spectrum from Proton-recoil Proportional Counters in Half-lethargy Groups	36
A.I.	Statistical Parameters for ^{239}Pu	37

EXPERIMENTAL RESULTS FOR ZPR-3 ASSEMBLIES 58 AND 59

by

J. M. Stevenson,* J. M. Gasidlo,
V. C. Rogers, G. G. Simons,
and R. O. Vosburgh

ABSTRACT

This report presents the results of measurements made on ZPR-3 Assemblies 58 and 59. These assemblies had a simple plutonium-graphite cell and differed in the reflector, which was depleted uranium (in Assembly 58) or lead (in Assembly 59). In particular, the experiments reported are critical mass, fission-rate and perturbation distributions, central fission ratios, central perturbations, the Doppler reactivity effect in a natural uranium oxide sample, and the central neutron spectrum by the proton-recoil method. Some of the experiments were performed in both assemblies, others in only one.

I. INTRODUCTION

The essential purpose of the construction of ZPR-3 Assemblies 58 and 59 was to study the apparently persistent discrepancy between calculated and measured central-reactivity worths. Nearly all the measurements made had some bearing on this discrepancy. The assemblies were constructed with a single-drawer core cell, which consisted of two plutonium-aluminum columns and 14 graphite columns, and which therefore formed a natural continuation of the series of the benchmark-physics assemblies (ZPR-3, Assemblies 48, 49, 50, 53, and 54). The two assemblies differed from each other in the reflector: Assembly 58 had a depleted-uranium reflector; Assembly 59 had a lead reflector. Thus the latter assembly was unusual in that it contained no uranium.

II. SELECTION OF ASSEMBLIES 58 AND 59

The objective of the benchmark series was to build a set of simple-geometry, simple-composition assemblies which would facilitate accurate postanalysis and provide an opportunity for evaluating calculational methods

*Visiting Scientist, United Kingdom Atomic Energy Authority, Winifrith, England.

and nuclear cross-section compilations. The first assemblies[1] contained plutonium, uranium, sodium, and steel as are found in a fast power reactor. Because of inventory limitations, only small assemblies with high fuel concentrations could be built; because of its cross-section simplicity, graphite was chosen to moderate the spectrum to be similar to that of a fast power reactor. The U/Pu ratio in these first assemblies was approximately 4.2. Later in the series, this ratio was reduced to about 1.5 by replacing the depleted-uranium plates by graphite and only leaving the uranium in the mixed plutonium-uranium fuel plates. In the later assemblies, the sodium was also replaced by graphite.

A final step was desirable, in which the plutonium-uranium fuel-plate columns were replaced by a second column of plutonium-aluminum fuel, producing a core drawer with no uranium and 95% ^{239}Pu in the plutonium and therefore strongly emphasizing the ^{239}Pu cross-section data in any analysis. In the absence of ^{238}U, with its strongly negative Doppler coefficient, earlier, less accurate, nuclear data did not initially satisfy the mandatory safety requirement that any plutonium assembly built on ZPR-3 had a calculated negative prompt-temperature coefficient. However, calculations with more recent ^{239}Pu data (which gave good predictions of a small sample plutonium Doppler measurement) showed that the proposed assembly did have a negative Doppler coefficient (see appendix, taken from Ref. 2), and the proposed assemblies were approved.

Analysis of experimental results of the previous assemblies in the series showed the now familiar discrepancy in the worth of central perturbation samples. To convert experimental perturbation measurements to units (dk/k) given by calculations requires a calculated value for β_{eff} that is a function of the delayed-neutron fractions for the various fissile isotopes. This calculated parameter has been considered a possible source of the error, and recent Los Alamos measurements have cast suspicion on the accepted values of the delayed-neutron fractions of ^{238}U.[3] This was an added reason for building the proposed assemblies, which had a β_{eff} containing no core contribution from ^{238}U. A system with a depleted-uranium reflector maintained the continuity of the series and also resulted in a β_{eff} with significant contribution, about 25%, from ^{238}U; the β_{eff} for a second system with a nonfissile reflector only involved the plutonium parameters. Comparison of the discrepancy for these two assemblies and the earlier ones in the series might indicate the accuracy of the accepted delayed-neutron fraction for ^{238}U. There is already other evidence suggesting that the ^{238}U data are consistent with those from the other isotopes[4] and that the ^{238}U data were not the likely source of the discrepancy.

The simple cell, containing only two materials, allowed simple changes to be made in the sample environment studies and also permitted less ambiguous cross-section preparation in the analysis of the assemblies.

Lead was used as the second reflector material because of its small capture cross section and its lesser moderating properties compared with other alternatives available, such as steel or graphite, which would modify the core spectrum more.

Experiments that had particular bearing on the central perturbation discrepancy were:

1. The influence of the environment on the central perturbation sample worths.
2. Traverses with fission counters and perturbation samples to give information relating to the perturbation denominators.
3. Californium-252 source perturbation traverses at known reactor power levels as part of the measurement of β_{eff} in Assembly 59.

The short time that ZPR-3 was available for Assemblies 58 and 59 restricted the number of experiments that could be carried out. Emphasis was placed on the above experiments, and only a few further measurements were made.

Whether the study was successful in achieving its objectives will not be apparent until after a detailed analysis and comparison of the calculated results and the experimental values.

III. ASSEMBLY COMPOSITIONS AND CRITICAL MASSES

The standard core-drawer loadings for Assembly 58 are shown in Fig. 1. A back drawer contained the other 8 in. of axial reflector for Half 1. The drawers for control and safety rods had an inside width of 1.875 in. and differed in that the odd graphite column in the core was missing, leaving a symmetrical loading. The asymmetric loading on the reactor matrix was used because the lead blocks for the reflector in Assembly 59 were available only in 4-in. lengths.

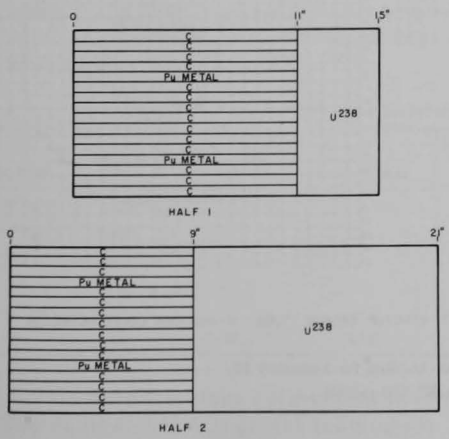

Fig. 1. Core Drawer Loading for Assembly 58. ANL Neg. No. ID-103-2990.

The critical loadings are shown in Figs. 2 and 3. The half-drawer in Assembly 59 was to keep the excess reactivity below the maximum allowed: 75¢. The numbers in the matrix positions refer to different drawer loadings, as in Table I. The compositions of the

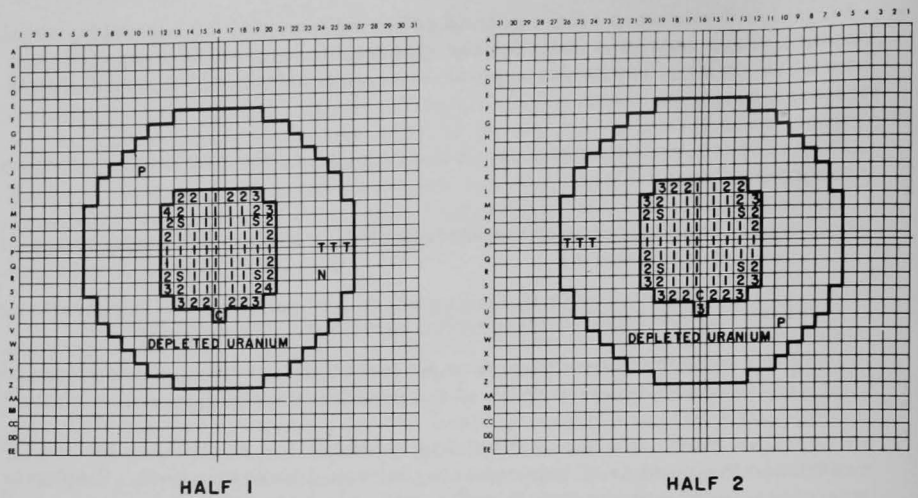

Fig. 2. Reference Core Loading for Assembly 58.
ANL Neg. No. ID-103-2988.

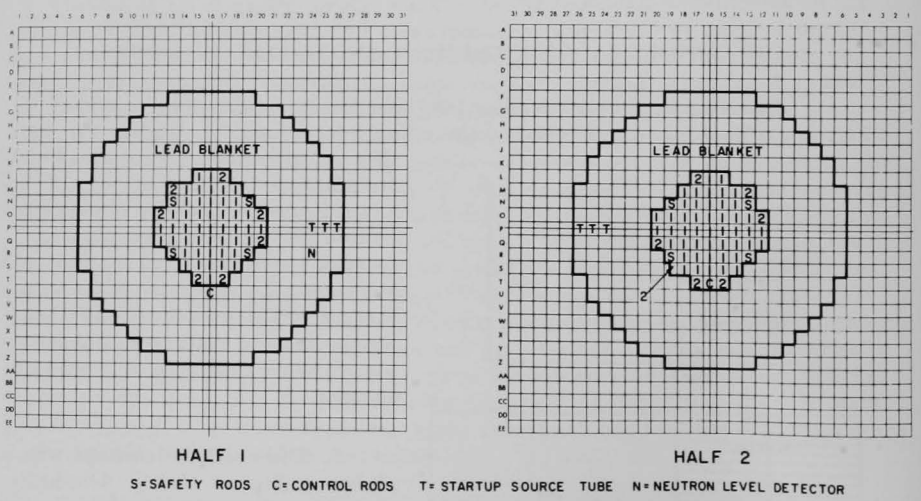

Fig. 3. Reference Core Loading for Assembly 59.
ANL Neg. No. ID-103-A2026.

TABLE I. Composition of Assembly 58

Region	Material Density, 10^{21} atoms/cm^3											
	^{239}Pu	^{240}Pu	^{241}Pu	Al	C	Fe	Cr	Ni	Mn	Si	^{238}U	^{235}U
Half 1 rods	2.1054	0.1005	0.0055	0.219	55.09	11.451	2.848	1.247	0.1189	0.1396	-	-
Type 1	2.1054	0.1005	0.0055	0.219	59.33	7.383	1.836	0.804	0.0767	0.0900	-	-
Type 2	2.1012	0.0994	0.0063	0.199	59.33	7.500	1.865	1.115	0.0779	0.0914	-	-
Type 3	2.0906	0.0994	0.0059	0.209	59.33	7.442	1.851	0.947	0.0773	0.0907	-	-
Type 4	2.1097	0.1000	0.0062	0.204	59.33	7.482	1.861	1.060	0.0777	0.0912	-	-
Type 5	2.1232	0.1006	0.0062	0.204	59.33	7.467	1.857	1.054	0.0775	0.0910	-	-
Half 2 rods	2.1012	0.1003	0.0055	0.219	55.11	11.512	2.863	1.253	0.1195	0.1403	-	-
Type 1	2.1012	0.1003	0.0055	0.219	59.35	7.401	1.841	0.806	0.0768	0.0902	-	-
Type 2	2.0972	0.0992	0.0063	0.198	59.35	7.516	1.869	1.115	0.0780	0.0916	-	-
Type 3	2.1072	0.0998	0.0063	0.203	59.35	7.500	1.865	1.067	0.0779	0.0914	-	-
Core average	2.1024	0.1001	0.0058	0.213	59.07	7.689	1.912	0.928	0.0798	0.0937	-	-
Radial reflector	-	-	-	-	-	4.540	1.129	0.494	0.0471	0.0553	38.71	0.086
Axial reflector	-	-	-	-	-	5.593	1.391	0.609	0.0581	0.0682	39.05	0.086
Spring gap	-	-	-	-	-	16.85	4.19	1.83	0.175	0.205	-	-

positions include the drawer fronts and are homogenized into lengths of 11.03 and 9.03 in. for Halves 1 and 2, respectively.

In both halves of both assemblies, core control and safety rods and Type 1 drawers contained plutonium-aluminum plates without an inner nickel cladding. Type 2 drawers contained nickel-clad plates, and the remainder contained both types of plates. The compositions were made very similar by suitable choice of the number of plates and therefore the number of gaps in the fuel columns. The small quantity of ^{242}Pu has been included in the ^{240}Pu. The ^{241}Pu contents have been corrected for decay (half-life, 13.2 years) since the analysis in 1960, and the low-worth daughter (^{241}Am) has been ignored.[5]

The average compositions for the core and reflector regions are given in Table I for Assembly 58 and Table II for Assembly 59. In both assemblies, the radial reflector blocks were loaded directly into the matrix tubes. The uranium-reflector compositions were somewhat different from those in previous ZPR-3 assemblies, as ZPPR blocks were used rather than ZPR-3 blocks.

TABLE II. Average Core and Reflector Compositions of Assembly 59

Material	Density, 10^{21} atoms/cm^3			Material	Density, 10^{21} atoms/cm^3		
	Core	Axial Reflector	Radial Reflector		Core	Axial Reflector	Radial Reflector
^{239}Pu	2.1030	-	-	Cr	1.919	1.391	1.129
^{240}Pu	0.1003	-	-	Ni	0.875	0.609	0.494
^{241}Pu	0.0056	-	-	Mn	0.0801	0.0581	0.0471
Al	0.217	-	-	Si	0.0941	0.0682	0.0553
C	59.02	-	-	Pb	-	28.16	28.24
Fe	7.717	5.593	4.540				

An equivalent cylindrical loading for Assembly 58 is shown in Fig. 4. The equivalent cylindrical loading for Assembly 59 differs only in the core radius, which was 23.83 cm. At the critical loadings, control rod 6 was

withdrawn 0.66 in. in Assembly 58 and control rod 5 was withdrawn 1.83 in. in Assembly 59. The fissile contents were 101.63 kg of ^{239}Pu and 0.28 kg of ^{241}Pu (Assembly 58) and 75.89 kg of ^{239}Pu and 0.20 kg of ^{241}Pu (Assembly 59). The amounts of excess reactivity and the corresponding corrections to the critical masses are considered in the next section.

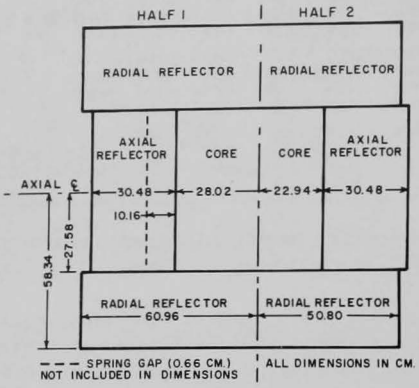

Fig. 4

Equivalent Cylindrical Dimensions for Assembly 58. ANL Neg. No. ID-103-2989.

IV. CALIBRATION OF SAFETY RODS, CONTROL RODS, AND AUTORODS

The worth of one safety rod in each half of the reactor and the worths of both control rods in each assembly were determined by inverse-kinetics techniques. (See Appendix B of Ref. 1.) The delayed-neutron parameters used are shown in Tables III and IV. The fractions were obtained from the Bailiff routine of the MACH-1 program,[6] using the delayed-neutron data of Keepin[7] and cross sections prepared as detailed in Ref. 2.

TABLE III. Delayed-neutron Data for Control-rod Calibrations

		Group Effective Delayed-neutron Fractions (units of 10^{-5})						
Assembly	Isotope	1	2	3	4	5	6	Total
58	^{235}U	0.129	0.724	0.639	1.383	0.435	0.088	3.398
	^{238}U	0.893	9.413	11.131	26.658	15.459	5.153	68.707
	^{239}Pu	7.214	53.157	41.007	62.270	19.554	6.645	189.847
	^{240}Pu	0.083	0.805	0.566	1.031	0.377	0.085	2.947
	^{241}Pu	0.057	0.418	0.322	0.489	0.154	0.052	1.491
								266.391
59	^{239}Pu	8.278	60.995	47.053	71.451	22.437	7.624	217.839
	^{240}Pu	0.094	0.919	0.646	1.178	0.431	0.098	3.365
	^{241}Pu	0.067	0.496	0.382	0.581	0.182	0.062	1.770
								222.974

Note: For Assembly 58, inhours/% ρ = 1065; for Assembly 59, inhours/% ρ = 1115.

TABLE IV. Group-decay Constants for Delayed Neutrons

Isotope	Decay Constants, sec^{-1}					
	1	2	3	4	5	6
^{235}U	0.0127	0.0317	0.115	0.311	1.40	3.87
^{238}U	0.0132	0.0321	0.139	0.358	1.41	4.02
$^{239}Pu + ^{241}Pu$	0.0129	0.0311	0.134	0.331	1.26	3.21
^{240}Pu	0.0129	0.0313	0.135	0.333	1.36	4.04

The effective source strengths were first determined by period measurements; then the rod-worth curves were obtained by fully withdrawing a single rod from a balanced reactor. The results are shown in Table V. In Assembly 58, the four safety-rod positions were symmetrical, so that the total worth of the eight safety rods was four times the sum of the worths of rods 3 and 7, i.e., 2.86% dk/k. In Assembly 59, rods 3 and 7 were some of the closest to the core-reflector interface, so that the total worth of the eight safety rods was more than four times that sum, i.e., 3.19% dk/k. In both cases, the total worth was significantly above that required by the reactor operating limits (1.5% dk/k).

TABLE V. Worths of Control and Safety Rods

Rod	Matrix Position	Assembly 58 Worth, % dk/k	Assembly 59 Worth, % dk/k
Safety 3	2-R-13	0.337	0.373
Safety 7	1-R-13	0.378	0.425
Control 5	2-T-16	0.314	0.330
Control 6	1-U-16	0.248	0.116
Total eight safety rods	-	2.860	>3.192

Note: These worths are for a stroke of 9.5 in.

The control-rod calibration curves enabled the excess reactivities of the loadings in Figs. 2 and 3 to be determined as 0.020% dk/k and 0.080% dk/k, respectively. Examination of the final stages of the approach-to-critical curves showed rod 6 was equivalent to 0.99 kg of edge fuel in Assembly 58 and rod 5 was equivalent to 0.95 kg of edge fuel in Assembly 59. Using the worth curves, the excess reactivities were converted to 0.07 and 0.22 kg of edge fuel, respectively.

In both assemblies, the autorod was placed in matrix position O-22 in the radial reflector. The autorod consisted of a tapered polyethylene wedge 0.25 in. thick, 72 in. long, and 1.75 and 0.25 in. high at the ends. In Assembly 58, the polyethylene wedge moved axially alongside the core

between 0.25-in. columns of boral; in Assembly 59, there was only one column of boral, on the core side of the wedge. The total worth of the autorod for the 20-in. stroke was obtained by inverse kinetics. Starting with the rod at its more reactive extremity in a balanced reactor, the rod was then oscillated in and out about five times (~13 sec stroke, ~27 sec wait). The results were 10.35 Ih in Assembly 58 and 19.41 Ih in Assembly 59. A standard error of ±1% is considered appropriate for all the uncertainties associated with the inverse-kinetics technique, but is not included in the perturbation results quoted in later sections of this report.

The differential worth of the autorod was measured by oscillating a sample (during the perturbation measurements below) between two positions which gave a reactivity change equal to about 10% of the autorod, and finding the variation of the resulting change in the rod position as a function of the rod position. This change varied by ~10% along the rod. The results were analyzed to give the relative reactivity change per unit movement along the rod and fitted to polynomial functions of the position. The best fit in both assemblies was a quadratic expression. The coefficients of the polynomial that gave reactivity against autorod position was obtained by integrating the differential worth and normalizing to the total worth.

V. FISSION-RATE DISTRIBUTIONS

Radial fission-rate distributions in Assembly 58 and both radial and axial fission-rate distributions in Assembly 59 were measured with ^{239}Pu and ^{238}U cylindrical fission chambers. Details of the counters are given in Table VI. The axial traverse tube was inserted through drawers where the plates had been rotated and special small graphite pieces used to leave a 0.5-in. square hole as shown in Fig. 5. For the radial traverses, the front 2 in. of all the Half 1 core drawers in row P were rotated and arranged in the same way. Thus Fig. 5 also represents a side view of the front 2 in. of these drawers. The remaining 9 in. of the plates were left in the usual vertical orientation. In the radial traverses, the counters, being ~1 in. back from the interface, were close to the core midplane, because of the asymmetric loading. Perforated blocks were used in the reflectors for all

TABLE VI. Traverse Counter Specifications

Main Isotope (Counter number)	Composition	Loading, mg	Plated length, in.
^{239}Pu (Q)	94.9 wt% ^{239}Pu 4.8 wt% ^{240}Pu 0.3 wt% ^{241}Pu	5.9	0.8
^{238}U (IC-24-4)	80 ppm ^{235}U	4.4	0.8

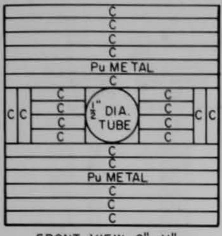

Fig. 5
Axial Traverse Drawer Loading in Half 1 of Assembly 59. ANL Neg. No. ID-03-A2014.

traverses. Discriminator settings for each counter were chosen from an integral bias curve. During each traverse, the reactor power was held constant using the autorod, and the counter was returned to the core center several times and counts taken at the reactor center to guard against reactor power or electronic drifts. No drifts were in fact observed. The results of the six traverses are shown in Tables VII-IX and Figs. 6-11. Two points are worth noting:

1. The radial traverses in both assemblies show a marked fine structure. The ^{239}Pu fission rate was higher when the counter straddled two drawers whereas the ^{238}U count rate was higher when the counter was centered on a drawer.

2. In Assembly 59, the ^{239}Pu radial traverse extended further than in Assembly 58, up to the core-radial reflector interface (P-20/21), where the count rate differed significantly from that at the equivalent position (P-11/12). This trend continued into the reflector, and the results in positions P-21 and P-22 were found to be a function of the autorod position. The count rate was several percent higher when the autorod polyethylene blade was almost fully inserted compared with the almost withdrawn position. Thus the discrepancy in the ^{239}Pu fission rate at position P-20/21 appears to be associated with the autorod in position O-22.

TABLE VII. Fission-Rate Radial Traverses in Assembly 58

	^{238}U		^{239}Pu	
Position	Relative Count Rate	Statistical Error, %	Relative Count Rate	Statistical Error, %
P-19	0.7154	0.6	0.7553	0.6
P-18/19	0.7730	0.6	0.8385	0.5
P-18	0.8680	0.5	0.8979	0.5
P-17/18	0.8997	0.5	0.9584	0.5
P-17	0.9568	0.5	0.9710	0.5
P-16/17	0.9631	0.5	1.0147	0.5
P-16	1.000	-	1.000	-
P-15/16	0.9615	0.5	1.0149	0.5
P-15	0.9672	0.5	0.9708	0.5
P-14/15	0.9037	0.5	0.9588	0.5
P-14	0.8695	0.5	0.8961	0.5
P-13/14	0.7879	0.6	0.8484	0.5
P-13	0.7187	0.6	0.7549	0.6
P-12/13	0.6059	0.6	0.6780	0.6
P-12	0.5049	0.6	0.5640	0.6
P-11/12	0.3380	0.8	0.4463	0.7
P-11	0.1852	1.1	0.3238	0.8
P-10	0.0628	1.3	0.1726	1.1
P-9	0.0231	1.5	0.0939	1.2
P-8	0.00933	1.7	0.0516	1.1
P-7	0.00351	2.2	0.0267	1.5
P-6	0.00131	3.6	0.0129	1.5

Horizontal matrix pitch is 2.1833 in.; core center is P-16.

TABLE VIII. Fission-rate Radial Traverses in Assembly 59

Position	^{239}Pu Relative Count Rate	^{239}Pu Statistical Error, %	^{238}U Relative Count Rate	^{238}U Statistical Error, %	Position	^{239}Pu Relative Count Rate	^{239}Pu Statistical Error, %	^{238}U Relative Count Rate	^{238}U Statistical Error, %
P-20/21	0.6431[a]	0.5	-	-	P-14	0.9046	0.4	0.8764	0.5
P-20	0.6432	0.5	0.5292	0.6	P-13/14	0.8680	0.5	0.7940	0.5
P-19/20	0.7309	0.5	0.6119	0.6	P-13	0.7806	0.5	0.7290	0.5
P-19	0.7728	0.5	0.7245	0.5	P-12/13	0.7319	0.5	0.6175	0.5
P-18/19	0.8568	0.5	0.7856	0.5	P-12	0.6474	0.5	0.5344	0.6
P-18	0.8885	0.4	0.8760	0.5	P-11/12	0.6113	0.5	0.3818	0.7
P-17/18	0.9592	0.4	0.9003	0.4	P-11	0.5769	0.5	0.2633	0.8
P-17	0.9733	0.4	0.9651	0.4	P-10	0.4736	0.6	0.1359	1.1
P-16/17	1.0096	0.4	0.9690	0.4	P-9	0.3799	0.7	0.0739	1.1
P-16	1.0000	-	1.0000	-	P-8	0.2908	0.8	0.0421	1.2
P-15/16	1.0199	0.4	0.9657	0.4	P-7	0.2069	0.9	0.0229	1.4
P-15	0.9786	0.4	0.9733	0.4	P-6	0.1266	1.2	0.0125	1.6
P-14/15	0.9620	0.4	0.9095	0.4					

[a]See text for explanation for high count rate at this position.

TABLE IX. Fission-rate Axial Traverses in Assembly 59

Distance from Centerline, in.	^{239}Pu Relative Count Rate	^{239}Pu Statistical Error, %	^{238}U Relative Count Rate	^{238}U Statistical Error, %	Distance from Centerline, in.	^{239}Pu Relative Count Rate	^{239}Pu Statistical Error, %	^{238}U Relative Count Rate	^{238}U Statistical Error, %
-10.06	0.6332	0.6	0.4119	0.7	+6.00	0.8598	0.5	0.8197	0.5
-9.06	0.6695	0.6	0.5502	0.6	+7.00	0.8127	0.5	0.7598	0.5
-8.06	0.7257	0.6	0.6519	0.6	+8.00	0.7452	0.5	0.6797	0.5
-7.06	0.7871	0.5	0.7364	0.5	+9.00	0.6804	0.6	0.5789	0.6
-6.06	0.8443	0.5	0.7987	0.5	+10.00	0.6517	0.6	0.4421	0.7
-5.06	0.8916	0.5	0.8734	0.5	+11.00	0.6272	0.6	0.3124	0.8
-4.06	0.9379	0.5	0.9111	0.5	+12.00	0.5820	0.6	0.2272	0.9
-3.06	0.9666	0.5	0.9570	0.5	+13.00	0.5333	0.6	0.1691	0.7
-2.06	0.9813	0.5	0.9781	0.5	+14.00	0.4883	0.6	0.1271	0.8
-1.03	0.9990	0.5	0.9837	0.5	+15.00	0.4431	0.7	0.1008	0.9
0	1.0000	-	1.0000	-	+16.00	0.4004	0.7	0.0755	0.8
+1.00	1.0000	0.5	0.9954	0.5	+17.00	0.3569	0.8	0.0576	0.9
+2.00	0.9962	0.5	0.9773	0.5	+18.00	0.3127	0.8	0.0443	1.0
+3.00	0.9757	0.5	0.9590	0.5	+19.00	0.2678	0.9	0.0334	1.2
+4.00	0.9420	0.5	0.9288	0.5	+20.00	0.2273	0.9	0.0254	1.3
+5.00	0.9104	0.5	0.8799	0.5	+21.00	0.1849	1.0	0.0184	1.5

Note: Centerline is 1.03 in. from the interface in Half 1. Positive numbers are in Half 1.

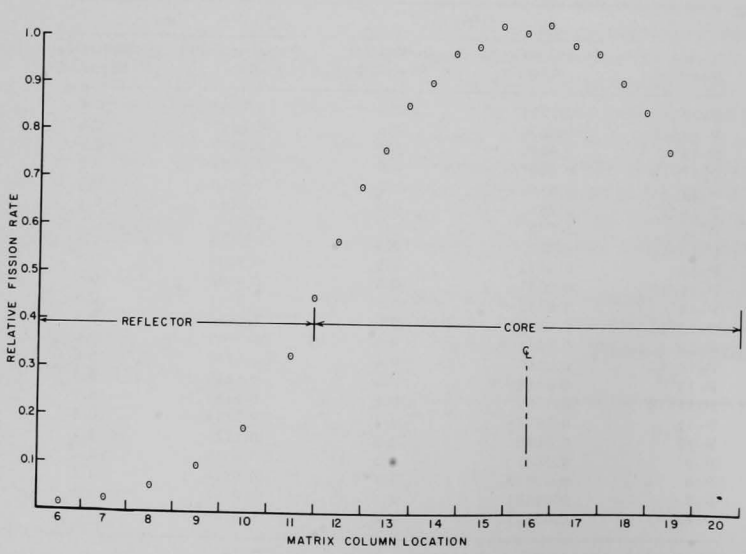

Fig. 6. ^{239}Pu Fission-rate Radial Traverse in Assembly 58. ANL Neg. No. ID-103-2994.

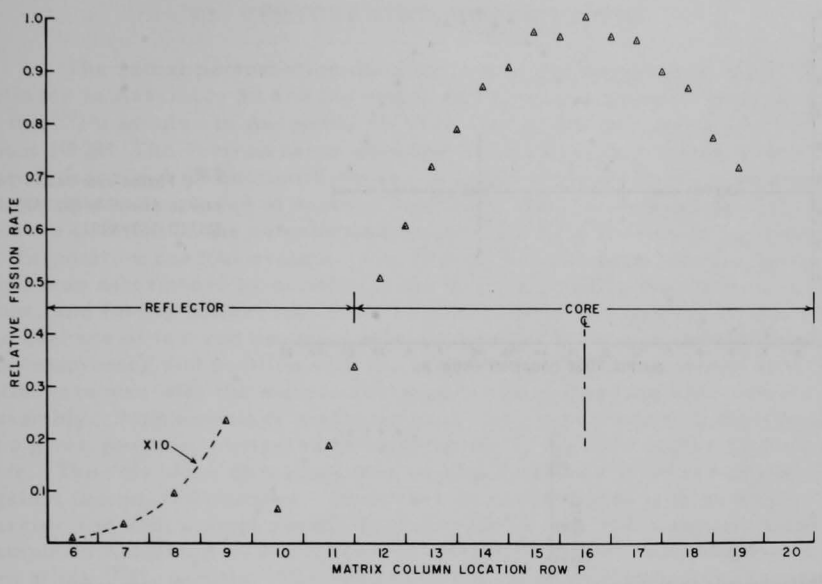

Fig. 7. ^{238}U Fission-rate Radial Traverse in Assembly 58. ANL Neg. No. ID-103-2993.

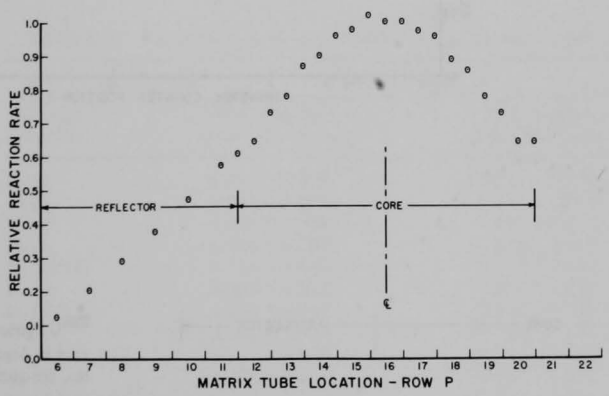

Fig. 8. ^{239}Pu Fission-rate Radial Traverse in Assembly 59. ANL Neg. No. ID-103-A2013.

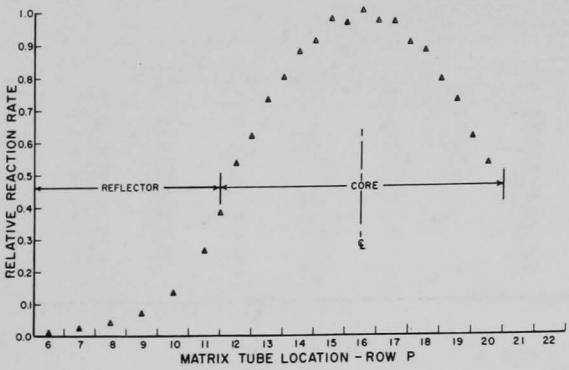

Fig. 9

^{238}U Fission-rate Radial Traverse in Assembly 59. ANL Neg. No. ID-103-A2011.

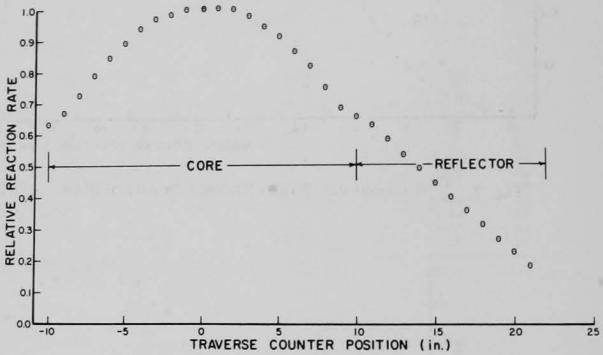

Fig. 10

^{239}Pu Fission-rate Axial Traverse in Assembly 59. ANL Neg. No. ID-103-A2012.

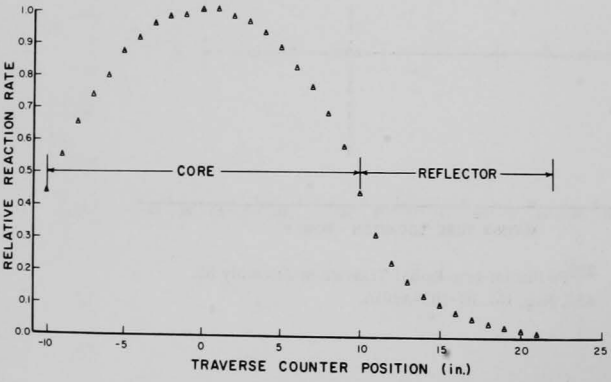

Fig. 11

^{238}U Fission-rate Axial Traverse in Assembly 59. ANL Neg. No. ID-103-A2010.

VI. PERTURBATION DISTRIBUTIONS

The radial perturbation distributions of a ^{239}Pu annulus and a ^{238}U cylinder in Assembly 58 and the radial and axial perturbation distributions of the ^{239}Pu annulus in Assembly 59 were measured, at a power level of about 10 W. The environments were the same as for the fission-rate traverses described in Section V above. A traverse drive mechanism allowed the sample to be placed at various positions. The corresponding critical balance position of the autorod was determined by a 100-sec integrated count of the position readout system. The reactivity difference between two positions was determined by oscillating the sample, reading the autorod positions, and finding differences from sets of three to correct for drifts; e.g., the average of two rod positions with the sample "out" was compared with the intervening rod position with the sample "in."[8] The reference reactivity difference was with the sample at the core center and then fully outside the assembly. Supplementary measurements were then made with the sample at a given position, compared to being either at the core center or fully outside. The reference difference was repeated during a traverse to guard against unexpected changes. Traverses were also made with an empty carrier and with a steel sample in Assembly 58 and with a dummy steel sample in Assembly 59 to correct for the worth of the carrier and the steel can of the ^{239}Pu sample. The results of the sample perturbation traverses are shown in Tables X and XI and Figs. 12-15. Because the samples are 2 in. long (almost the length of the horizontal unit cell), no fine structure is seen in the radial traverses.

TABLE X. Perturbation Radial Traverses in Assembly 58

Matrix Position	Sample Worth, Ih	
	^{239}Pu Annulus, 0.010 in. Thick	^{238}U Cylinder, 0.2 in. Diameter
P-19	2.797 ± 0.019	-0.452 ± 0.044
P-18	3.509 ± 0.017	-0.967 ± 0.019
P-17	4.020 ± 0.016	-1.270 ± 0.014
P-16	4.216 ± 0.012	-1.384 ± 0.013
P-15/16	4.130 ± 0.015	-1.373 ± 0.019
P-15	3.981 ± 0.015	-1.304 ± 0.015
P-14/15	3.747 ± 0.019	-1.156 ± 0.020
P-14	3.482 ± 0.019	-0.959 ± 0.017
P-13/14	3.115 ± 0.020	-0.733 ± 0.017
P-13	2.758 ± 0.015	-0.489 ± 0.017
P-12/13	2.403 ± 0.014	-0.195 ± 0.014
P-12	2.111 ± 0.016	+0.129 ± 0.017
P-11/12	1.715 ± 0.016	+0.342 ± 0.015
P-11	1.244 ± 0.015	+0.348 ± 0.016
P-10	0.463 ± 0.009	+0.090 ± 0.021
P-9	0.171 ± 0.010	+0.040 ± 0.010

Note: Errors quoted are standard errors calculated from spread of perturbation results. Sample details are given in Table XIV.

TABLE XI. Plutonium-239 Perturbation Traverses in Assembly 59

Radial		Axial	
Position	Sample[a] Worth,[b] Ih	Distance from Centerline, in.[c]	Sample[a] Worth,[b] Ih
P-20	2.054 ± 0.016	-10.06	1.646 ± 0.028
P-19	3.110 ± 0.043	-9.06	2.209 ± 0.019
P-18	4.168 ± 0.016	-8.06	2.709 ± 0.024
P-17/18	4.546 ± 0.032	-7.06	3.264 ± 0.032
P-17	4.964 ± 0.019	-6.06	3.687 ± 0.024
P-16/17	5.090 ± 0.020	-5.06	4.094 ± 0.026
P-16	5.225 ± 0.014	-4.06	4.457 ± 0.021
P-15/16	5.083 ± 0.024	-3.06	4.775 ± 0.025
P-15	4.963 ± 0.020	-2.06	5.020 ± 0.021
P-14/15	4.590 ± 0.026	-1.03	5.155 ± 0.030
P-14	4.203 ± 0.030	0	5.193 ± 0.014
P-13/14	3.652 ± 0.026	1.00	5.187 ± 0.020
P-13	3.110 ± 0.015	2.00	5.058 ± 0.030
P-12/13	2.533 ± 0.020	3.00	4.834 ± 0.025
P-12	1.996 ± 0.031	4.00	4.504 ± 0.058
P-11/12	1.564 ± 0.028	5.00	4.074 ± 0.027
P-11	1.139 ± 0.035	6.00	3.603 ± 0.021
P-10/11	0.920 ± 0.036	7.00	3.196 ± 0.044
P-10	0.669 ± 0.028	8.00	2.635 ± 0.028
P-9	0.377 ± 0.021	9.00	2.106 ± 0.025
P-8[d]	0.239 ± 0.026	10.00	1.572 ± 0.023
P-7[d]	0.076 ± 0.039	11.00	1.157 ± 0.043
		13.00	0.764 ± 0.028
		15.00	0.450 ± 0.028
		17.00	0.184 ± 0.036

[a]0.010-in.-thick ^{239}Pu annulus used.
[b]Errors quoted are standard errors calculated from spread of perturbation results.
[c]Positive numbers are into Half 1. Centerline is 1.03 in. into Half 1 from interface.
[d]Positions P-8 and P-7 were centered 0.25 in. in towards the core from the true cell center.

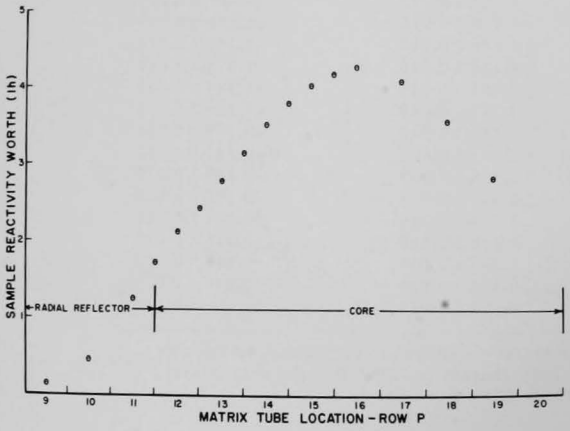

Fig. 12
^{239}Pu Perturbation Radial Traverse in Assembly 58. ANL Neg. No. ID-103-A2009.

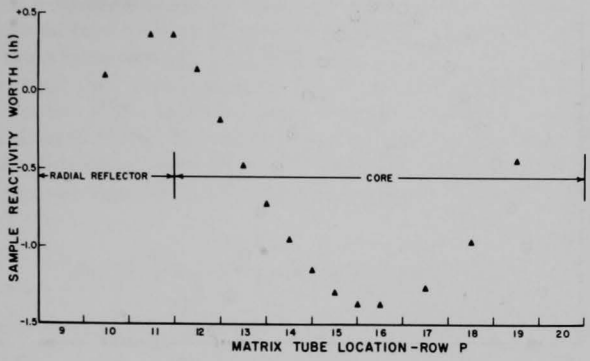

Fig. 13. ^{238}U Perturbation Radial Traverse in Assembly 58. ANL Neg. No. ID-103-A2008.

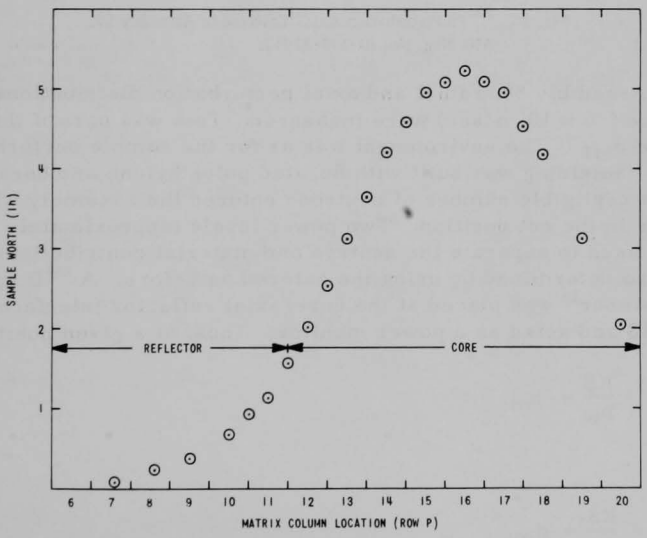

Fig. 14. ^{239}Pu Perturbation Radial Traverse in Assembly 59. ANL Neg. ID-103-A2018.

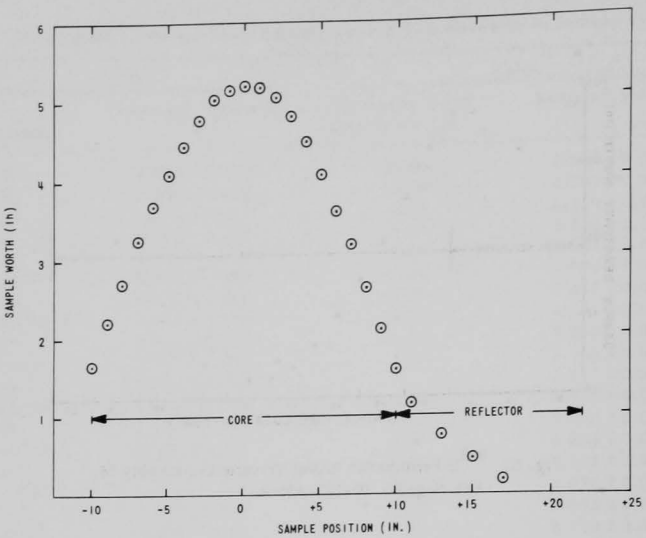

Fig. 15. ^{239}Pu Perturbation Axial Traverse in Assembly 59.
ANL Neg. No. ID-103-A2017.

In Assembly 59, radial and axial perturbation distributions with a ^{252}Cf source (~6 x 10^7 n/sec) were measured. This was part of the determination of β_{eff}.[9] The environment was as for the sample perturbation traverses. Shielding was built with borated polyethylene and boral to ensure that a negligible number of neutrons entered the assembly when the source was in the out position. Two power levels (approximately 50 and 8 W) were used to separate the neutron and material contributions. The worths were determined by using the autorod as before. A ^{235}U Kirn-type fission chamber[10] was placed at the core/axial reflector interface in position 2-M-18 and acted as a power monitor. Thus, at a given position,

$$\rho_{50} = \frac{KS}{n_{50}} + \rho_m,$$

and

$$\rho_8 = \frac{KS}{n_8} + \rho_m,$$

where ρ = reactivity, S = source strength, n = count rate on ^{235}U fission counter, ρ_m = material reactivity, and K = constant. Hence,

$$\rho_8 - \rho_{50} = KS\left(\frac{1}{n_8} - \frac{1}{n_{50}}\right).$$

Thus the reactivity difference is that of the source neutrons when the fission count rate is $n = n_{50} \cdot n_8/(n_{50} - n_8)$. This equivalent count rate was determined for the measurements at every point, and the reactivity differences were normalized to a chosen count rate using the fact that the worth of the source neutrons is inversely proportional to the count rate. A later measurement allowed this count rate on the ^{235}U chamber to be converted to the fission rate on the ^{239}Pu foil in a back-to-back chamber. The foil was 108.9 μg (94.4 wt % ^{239}Pu, 5.3 wt % ^{240}Pu, and 0.3 wt % ^{241}Pu), positioned 2 in. back from the interface in 2-P-16. The fission rate in this foil of 632.1 fissions/sec applies to all the source worths shown in Table XII and Figs. 16 and 17.

TABLE XII. Californium-252 Source Perturbation Traverses in Assembly 59

Radial		Axial		Radial		Axial	
Position	Source[a] Worth,[b] Ih	Position, in.[c]	Source[a] Worth,[b] Ih	Position	Source[a] Worth,[b] Ih	Position, in.[c]	Source[a] Worth,[b] Ih
P-20/21	4.937 ± 0.020	-10.06	5.112 ± 0.026	P-14	8.746 ± 0.034	+2.00	9.583 ± 0.026
P-20	5.950 ± 0.045	-9.06	6.004 ± 0.023	P-13/14	8.047 ± 0.023	+4.00	9.076 ± 0.023
P-19/20	6.656 ± 0.040	-8.06	6.795 ± 0.026	P-13	7.439 ± 0.022	+5.00	8.678 ± 0.024
P-19	7.579 ± 0.034	-7.06	7.447 ± 0.035	P-12/13	6.649 ± 0.028	+6.00	8.158 ± 0.030
P-18/19	8.106 ± 0.023	-6.06	8.134 ± 0.036	P-12	5.865 ± 0.032	+7.00	7.533 ± 0.031
P-18	8.702 ± 0.019	-5.06	8.590 ± 0.024	P-11/12	4.928 ± 0.036	+8.00	6.865 ± 0.025
P-17	9.589 ± 0.056	-4.06	8.997 ± 0.029			+9.00	6.128 ± 0.023
P-16	9.833 ± 0.014	-2.06	9.550 ± 0.027			+10.00	5.250 ± 0.027
P-15	9.578 ± 0.035	0	9.748 ± 0.022				

[a]Source strength for radial results (Jan. 2, 1970) = 5.955×10^7 n/sec; source strength for axial results (Jan. 7, 1970) = 5.933×10^7 n/sec.
[b]All results at a power such that ^{239}Pu (94.4 wt % ^{239}Pu, 108.9 μg) foil in back-to-back chamber, 2 in. from the reactor interface in 2-P-16, undergoes 632.1 fissions/sec. Errors quoted are standard errors calculated from spread of perturbation results.
[c]Positive numbers are into Half 1. Center is 1.03 in. in Half 1 from interface.

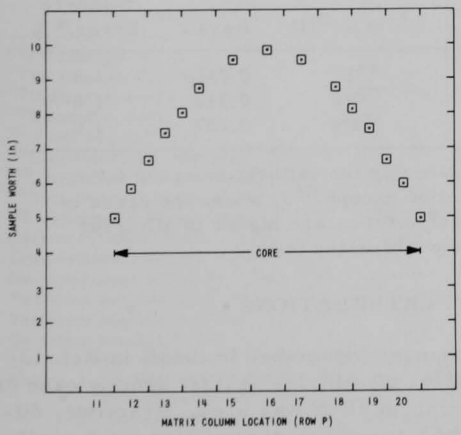

Fig. 16. ^{252}Cf Source-perturbation Radial Traverse in Assembly 59. ANL Neg. No. ID-103-A2020.

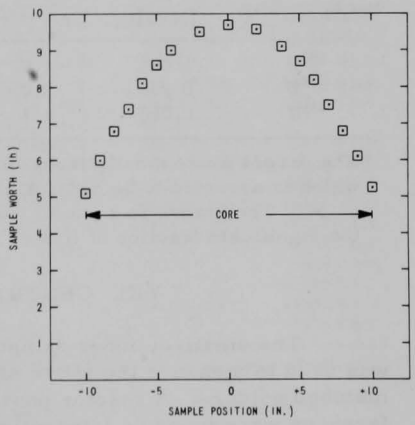

Fig. 17. ^{252}Cf Source-perturbation Axial Traverse in Assembly 59. ANL Neg. No. ID-103-A2019.

VII. CENTRAL FISSION RATIOS

Thin-walled, aluminum, spherical, back-to-back fission counters[11] were used in Assembly 59. The counters were positioned at the center of the cavity shown in Fig. 18, in position 1-P-16. Thus the foils (which were in a horizontal orientation) were extremely close to the core center. Each foil was paired with a ^{235}U foil. Counts were taken on a pulse-height analyzer (RIDL 34-12B) from each foil in turn for a suitable integrated live-time. The total fission pulses were added and a correction (generally ~1/2%) made for fission fragments lost in the noise and α-pulses. The corrections for fragments completely absorbed in the very thin films were small (<0.5%), similar, and cancelling and were therefore ignored. The corrected count-rate ratios were converted to fission ratios by a computer code which solved the simultaneous equations involving the numbers of atoms of each isotope in the foils. The results are shown in Table XIII.

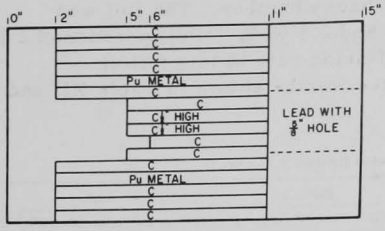

Fig. 18. Core Drawer for Back-to-Back Fission Counter. ANL Neg. No. ID-103-A2006.

TABLE XIII. Central Fission Ratios in Assembly 59

Ratio to ^{235}U	Result	Standard Error,[a] %	Ratio to ^{235}U	Result	Standard Error,[a] %
^{233}U	1.466	1.0	^{238}U	0.0325	1.8
^{234}U	0.183	2.0	^{239}Pu	0.942	1.0
^{236}U	0.068	1.7	^{240}Pu	0.207	1.0

[a]The errors arise mostly from uncertainty in the calibration of the foils, which is assumed to be ~1% for all ratios except ^{238}U, where the error is ~1.5%. The errors in some of the fission ratios are higher to allow for the significant fraction of fission in the ^{235}U in the foils.

VIII. CENTRAL PERTURBATIONS

The small-cylinder sample changer (described in detail in Ref. 12) was used to measure the worth of series of samples against dummy cans or matched holders. A reactor power of about 10 W was used. Reactivity differences were found by integrating the autorod balance position, as described in Section VI. Trials showed that the experimental results were the most reliable with a quick change (~2 sec) between sample and dummy positions and then a 100-sec wait before starting the 100-sec averaging of the position. The worth of the empty changer was also determined and sample results corrected accordingly. The standard environment, used in both assemblies was used for the radial traverses (described in Section V).

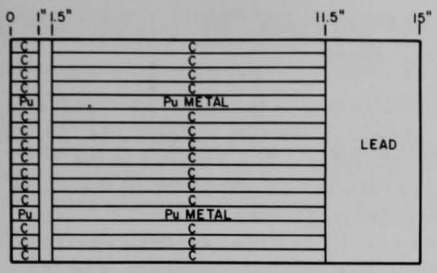

Fig. 19. Half-inch Voided Drawer for Central Perturbations. ANL Neg. No. ID-103-A2007.

A voided environment, seen in top view in Fig. 19, was also used in Assembly 59. The three central drawers contained this loading. The small graphite pieces in the other core drawers in the P row were adjusted to permit the traverse tube to be moved 0.25 in. further from the interface. The holes in the lead blocks were also moved. The samples were centered at the drawer half-height as in the standard environment.

The three sets of results are given in Table XIV. Agreement is seen between the central perturbations of the 0.010-in.-thick ^{239}Pu annulus and the 0.2-in.-diam ^{238}U cylinder in Assembly 58 (4.204 ± 0.008 Ih and -1.413 ± 0.011 Ih, respectively) and the values at the central positions of the radial traverses above. Similarly, the central perturbation in the standard environment in Assembly 59 for the

TABLE XIV. Central Perturbation Results

Sample	Mass, g	Sample Worth, Ih/kg: Assembly 58, Standard Environment	Assembly 59, Standard Environment	Assembly 59, Voided Environment
^{239}Pu annulus, 0.010 in.	4.801	875.7 ± 1.7	1100 ± 3	1025 ± 4
^{239}Pu annulus, 0.007 in.	2.761	862.0 ± 2.9	1076 ± 7	1007 ± 5
^{235}U annulus, 0.010 in.	7.128	566.4 ± 1.6	709.0 ± 2.8	665.0 ± 2.2
^{235}U annulus, 0.005 in.	3.638	552.4 ± 1.1	691.0 ± 3.6	653.1 ± 5.5
^{235}U annulus, 0.003 in.	2.327	554.0 ± 3.4	696.6 ± 4.6	-
^{238}U cylinder, 0.42-in. diam	85.76	-54.8 ± 0.1	-61.3 ± 0.2	-65.0 ± 0.2
^{238}U cylinder, 0.20-in. diam	19.63	-72.0 ± 0.5	-82.0 ± 1.3	-85.4 ± 0.7
^{238}U cylinder, 0.10-in. diam	4.908	-88.3 ± 2.0	-104.1 ± 2.9	-108.6 ± 4.3
^{10}B cylinder, 0.06-in. diam	0.0988	-39710 ± 110	-49230 ± 180	-48710 ± 190
Carbon cylinder, 0.4-in. diam	6.910	-	333.4 ± 3.2	319.2 ± 1.9
Lead cylinder, 0.4-in. diam	51.36	-	-	6.9 ± 0.3
Stainless steel cylinder, 0.4-in. diam	35.90	-	-	4.9 ± 0.6
Tantalum annulus, 0.005 in.	3.300	-	-	-1205 ± 5
Tantalum annulus, 0.003 in.	1.888	-	-1322 ± 13	-1302 ± 6
Tantalum annulus, 0.002 in.	1.317	-	-	-1374 ± 8

Notes: 1. Errors quoted are standard errors calculated from spread of inhour determinations. Not included are errors in sample masses.

2. All samples are 2 in. long. The annuli have outside diameters of approximately 0.40 in.

3. Sample compositions:

^{239}Pu: 98.78 wt % Pu; 95.05 wt % ^{239}Pu, 4.50 wt % ^{240}Pu, 0.45 wt % ^{241}Pu

^{235}U: 0.010-in. annulus, 93.20 wt % ^{235}U; others, 93.10 wt % ^{235}U

^{238}U: 0.21 wt % ^{235}U

^{10}B: 92.8 wt % boron, 92.1 wt % ^{10}B in boron

Others: No significant contaminants.

0.010-in.-thick ^{239}Pu annulus (5.281 ± 0.016 Ih) agrees satisfactorily with the center points of the radial and axial traverses.

Ratios of results from Table XIV are listed in Table XV. The ratio of perturbations in the standard environment in the two assemblies (59/58) is a constant for the ^{239}Pu, ^{235}U, and ^{10}B samples. The ratios for the ^{238}U cylinders are somewhat less. A similar difference, about 5% in the same direction, was found in the design calculations, for zero-size ^{238}U.[2] The differences in Assembly 59 between the results for the standard environment, where the samples were in a graphite-modified spectrum, and the voided environment, where the samples saw an approximate cell average spectrum, demonstrate the perturbation uncertainties associated with the sample position chosen.

TABLE XV. Ratios[a] of Central Perturbations

Sample	Assembly 59, Standard Environment / Assembly 58, Standard Environment	Assembly 59, Voided Environment / Assembly 59, Standard Environment
^{239}Pu annulus, 0.010 in.	1.256 ± 0.004	0.932 ± 0.005
^{239}Pu annulus, 0.007 in.	1.248 ± 0.010	0.936 ± 0.009
^{235}U annulus, 0.010 in.	1.252 ± 0.006	0.938 ± 0.005
^{235}U annulus, 0.005 in.	1.251 ± 0.006	0.945 ± 0.009
^{235}U annulus, 0.003 in.	1.257 ± 0.012	-
^{238}U cylinder, 0.42-in. diam	1.118 ± 0.004	1.060 ± 0.004
^{238}U cylinder, 0.2-in. diam	1.139 ± 0.018	1.041 ± 0.017
^{238}U cylinder, 0.1-in. diam	1.180 ± 0.044	1.043 ± 0.049
^{10}B cylinder, 0.06-in. diam	1.240 ± 0.005	0.989 ± 0.005
Carbon cylinder, 0.4-in. diam	-	0.957 ± 0.012
Tantalum annulus, 0.003 in.	-	0.985 ± 0.011

[a]These ratios were obtained from the sample worths, measured in inhours, in the two environments. The errors quoted are standard errors calculated from the spread of the perturbation measurements. In the comparison of the standard environments in the two assemblies, systematic errors of 1% from the autorod calibration in each assembly must be added.

IX. CENTRAL SUBSTITUTION MEASUREMENTS

The reactivity worths of various alterations to the front of the core drawer in matrix position P-16 in Half 1 of Assembly 59 were measured. The reactor was shut down for each alteration. The changes in reactivity were determined from the balance positions of control rod 5. Temperature readings on 10 thermocouples attached to the reactor matrix were taken at

each balance. Reference loadings (with the plate arrangement in the core drawer chosen to make the substitution simple) were repeated before and after each substitution experiment, and the change in the average temperature allowed a temperature coefficient to be obtained to correct each result for drifts. Four determinations gave similar coefficients of about -2.5 Ih/°C. Temperature changes of about 1°C between successive closures of the reactor halves were observed. Thus the corrections applied to the measured reactivity effects were only a few inhours, with uncertainties <1 Ih.

The actual substitutions and the reactivity changes are detailed in Table XVI. For the last substitution experiment (the replacement of two 2-in. fuel plates by four 1-in. fuel plates), the front 2 in. of each set of core

TABLE XVI. Reactivity Worth of Central Substitution Experiments in Assembly 59

Substitution (in 1-P-16)	Changes in Mass, g		Reactivity, Ih
Remove one 2 x 1 x 1/8-in. plutonium plate and seven 2 x 1 x 1/8-in. carbon plates (i.e., front 1 in. of half a drawer).	^{239}Pu	-30.64	-46.3 ± 2.0
	^{240}Pu	-1.43	
	^{241}Pu	-0.08	
	Aluminum	-0.37	
	Steel	-9.37	
	Nickel	-1.2	
	Carbon	-40.406	
Replace front 2 in. of central column of graphite by 2 x 2 x 1/8-in. ^{10}B plate (i.e., midway between fuel plates).	^{10}B	+3.1	-144.7 ± 2.0
	^{11}B (+ impurities)	+0.5	
	Steel	+33.3	
	Carbon	-13.1	
Replace front 2 in. of central column of graphite by four 1 x 1 x 1/8-in. ^{235}U plates.	^{235}U	+133.77	103.4 ± 2.0
	^{238}U	+9.67	
	Carbon	-13.1	
Replace front 2 in. of central column of graphite by 2 x 2 x 1/8-in. plutonium plate.	^{239}Pu	+65.72	77.7 ± 2.0
	^{240}Pu	+3.18	
	^{241}Pu	+0.18	
	Aluminum	+0.76	
	Steel	+16.77	
	Carbon	-13.1	
Replace two front 2 x 2 x 1/8-in. ^{239}Pu plates by four 2 x 1 x 1/8-in. ^{239}Pu plates (using boxes).	^{239}Pu	-9.05	-10.0 ± 0.2
	^{240}Pu	-0.44	
	^{241}Pu	-0.01	
	Aluminum	-0.07	
	Steel	+1.54	
	Carbon	+0.08	

Note: For discussion of errors, see text.

material were loaded into small 2-in.-cube boxes to prevent movement of the rest of the contents of matrix position 1-P-16 (loaded in a standard 21-in. drawer). The two boxes were interchanged for the measurement. Table XVI includes the small differences in the graphite plate and steel box masses as well as the changes in the fuel-plate masses.

The errors in Table XVI arise from estimates of the uncertainties in (1) the temperature corrections, (2) the effect of opening and closing the reactor halves, and (3) the repositioning of the drawers. Whereas the other perturbed measurements were made only once, the boxes were interchanged several times (and only the front 2 in. were moved)--hence the significantly reduced error for the last measurement. The error in the autorod calibration (~1%) is not included.

X. DOPPLER REACTIVITY EFFECT OF NATURAL URANIUM OXIDE

The temperature coefficient of reactivity for a single 6-in. natural UO_2 sample was measured at the center of Assembly 59. (The rod traverse mechanism has been described in detail in Ref. 13.) The annular sample has an inner radius of 0.16 cm and an outer radius of 0.63 cm. The mass of UO_2 is 137.2 g. The drawer through which the traverse mechanism passes is shown in Fig. 20.

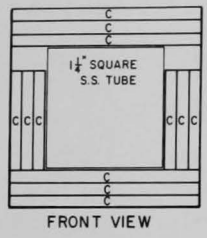

Fig. 20
Core Drawer for Doppler Sample in Assembly 59. ANL Neg. No. ID-103-A2016.

The total worth of the single sample (used because of the short core height) was measured at cell temperature by traversing the mechanism with an empty capsule and later with the sample in position, and noting the balance positions on Control Rod 5. The value obtained was -9.34 ± 0.09 Ih. The loading in the intermediate trays of the traverse rod was adjusted so that the movement of the rod induced only a fairly small change of the autorod position to maintain criticality throughout the movement. Measurements were made at about 10 W with the sample at approximately 300, 500, 800, and 1100°K. The technique for determining the reactivity change was similar to that in the central perturbation measurements (discussed in Section VIII). After an 80-sec wait, the autorod position was averaged over 160 sec for each traverse-rod position. Because of the extra core drawers added to maintain criticality, the autorod total worth was remeasured and found to be 19.76 Ih, compared with the previous value of 19.41 Ih. This higher worth was used in interpreting the measurements. The differential shape was assumed to be unchanged. The results of the measurements with no corrections for expansion effects applied are given in Table XVII.

TABLE XVII. Reactivity Changes of Natural UO_2 Sample

Temperature, °K	Reactivity Change, Ih
295	0
500	-0.994 ± 0.014
800	-1.980 ± 0.010
1099	-2.765 ± 0.007

Note: Errors quoted are standard errors calculated from the spread of the perturbation measurements only.

XI. CENTRAL NEUTRON SPECTRUM USING PROTON-RECOIL COUNTERS

The fast-neutron spectrum was measured over the energy range of 0.33 keV to 2.37 MeV near the center of Assembly 58. A hydrogen and methane cylindrical proportional counter, positioned with their centers of active volumes 4 in. from the reactor interface, were used in a voided drawer in matrix position 1-P-16. Figure 21 shows the drawer containing the hydrogen counter and preamplifier. (The basic spectrometer system has been described in Refs. 14 and 15.) Neutron-induced and (background) gamma-ray-induced pulses were separated by pulse rate-of-rise information. To keep the fraction of the latter to a minimum, the measurements were made before the assembly had been run at power, and the counters were enclosed in a 1/4-in.-thick lead sleeve.[15] The count rate from both sources at the critical configuration (Fig. 2) with all the control and safety rods withdrawn was greater than those acceptable for proper operation of the spectrometer system. Therefore some of the outermost core drawers

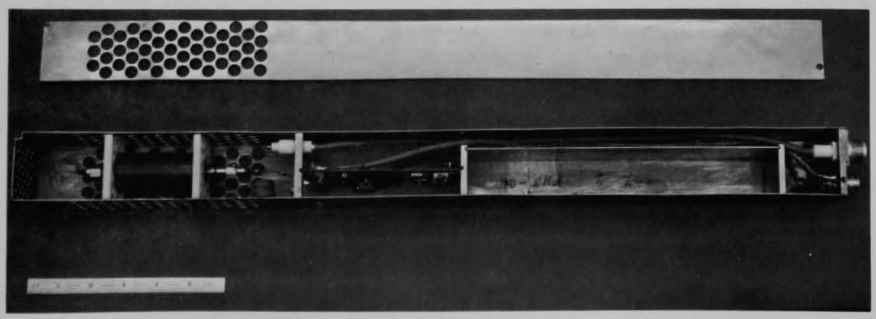

Fig. 21. 0.625-in.-diam Hydrogen Proportional Counter and Preamplifier Installed in Special Drawer. ANL Neg. No. ID-103-A11293.

were removed from the reactor and replaced by radial reflector drawers. The core outline at the loading used contained 70 matrix positions in Half 1 and 69 matrix positions in Half 2. The measurements were made with no core material in position 1-P-16, and all the control and safety rods withdrawn, i.e., at close to 7% dk/k subcritical.

The electronics used was a basic two-parameter system operating with the Data Machines 622 computer. No pulse-pileup circuitry was used. The reactor loading described above was chosen to give count rates of less than 6,000 counts per second, ensuring that pulse pileup would not distort the spectrum.

Two counters were required to cover the desired neutron-energy range. A 5-atm total-pressure hydrogen-filled counter 1.5 cm in diameter, with a 3.2-cm sensitive length and a 0.7-mil anode, was used from 0.33 to 120 keV. Data were obtained with the hydrogen counter using seven high-voltage settings at 200-V intervals beginning at 2800 V. A 5-atm total-pressure methane-filled 2.54-cm-diam counter with a 7.6-cm sensitive length and a 0.7-mil anode was used from 90 keV to 2.37 MeV. High-voltage settings of 3100, 3500, and 3800 V were required. The 30-keV energy overlap between the two counters ensured that the data from the two counters were properly normalized. Also, an approximately 30% overlap existed for each of the seven hydrogen-counter data sets and for each of the three methane-counter data sets.

Both the hydrogen and the methane counters were calibrated in the Argonne Fast Source Reactor (AFSR) thermal column just before the Assembly 58 fast-neutron spectrometer measurement. This was a standard calibration procedure, which used the protons from the $^{14}N(n, p)^{14}C$ reaction induced by thermal neutrons in the nitrogen gas within the detector chambers to determine a relationship between gas multiplication and voltage for each counter. An effective energy-shift factor of 0.95 was applied to the hydrogen calibration data to correct these data for pulse clipping occurring in the linear amplifier. (This factor was previously determined experimentally.[16]) Also, the electron-volt loss per ion pair was assumed constant for both counters. The methane cutoff energy was assumed to be 4 keV.

The proton-recoil data were analyzed using the ZPPR 840MP Computer version of the PSNS code.[17] Table XVIII and Fig. 22 show the resultant fast-neutron spectrum obtained using a slope-taking interval of 0.08 plus 0.120 times the reciprocal square root of the energy in keV. The uncertainties in the fluxes in Table XVIII and Fig. 22 include only statistical errors related to the analysis of the proton data.[15] Systematic errors in the neutron spectrum exist below 8 keV due to the energy dependence of the proton energy loss per ion pair created (W). This error, whose magnitude may exceed 10%, can be removed only after W for hydrogen below

TABLE XVIII. Neutron Spectrum from Proton-recoil Proportional Counters

INDEX	NEUTRØN ENERGY (KEV)	FLUX / UNIT LETHARGY	FLUX ERRØR
1	2,36972E 03	7,02182E 02	1,26688E 01
2	2,25687E 03	8,53186E 02	1,43115E 01
3	2,14940E 03	9,70583E 02	1,44378E 01
4	2,04705E 03	1,08746E 03	1,59362E 01
5	1,94957E 03	1,17667E 03	1,72299E 01
6	1,85674E 03	1,29303E 03	1,85140E 01
7	1,76832E 03	1,38318E 03	1,99206E 01
8	1,68411E 03	1,42386E 03	1,94304E 01
9	1,60392E 03	1,49535E 03	2,09832E 01
10	1,52754E 03	1,52864E 03	2,21893E 01
11	1,45480E 03	1,61026E 03	2,15003E 01
12	1,38552E 03	1,64481E 03	2,03205E 01
13	1,31955E 03	1,66031E 03	2,16299E 01
14	1,25671E 03	1,66816E 03	2,04576E 01
15	1,19687E 03	1,64636E 03	2,15769E 01
16	1,13987E 03	1,64720E 03	2,03125E 01
17	1,08560E 03	1,62051E 03	2,15886E 01
18	1,03390E 03	1,65986E 03	1,68681E 01
19	9,84667E 02	1,65081E 03	1,77039E 01
20	9,37778E 02	1,62575E 03	1,68447E 01
21	8,93122E 02	1,59449E 03	1,79013E 01
22	8,50592E 02	1,56672E 03	2,78028E 01
23	8,10088E 02	1,49821E 03	2,79864E 01
24	7,71512E 02	1,49320E 03	2,82761E 01
25	7,34773E 02	1,61101E 03	2,87805E 01
26	6,99784E 02	1,61119E 03	2,91665E 01
27	6,66461E 02	1,58675E 03	2,70069E 01
28	6,34725E 02	1,56307E 03	2,77353E 01
29	6,04500E 02	1,52249E 03	2,86009E 01
30	5,75714E 02	1,49109E 03	2,62860E 01
31	5,48299E 02	1,46461E 03	2,41788E 01
32	5,22190E 02	1,51096E 03	2,52960E 01
33	4,97324E 02	1,51987E 03	2,64549E 01
34	4,73642E 02	1,46983E 03	2,44375E 01
35	4,51087E 02	1,36667E 03	2,22786E 01
36	4,29607E 02	1,35101E 03	2,37216E 01
37	4,09149E 02	1,37531E 03	2,20090E 01
38	3,89666E 02	1,34720E 03	2,01506E 01
39	3,71111E 02	1,26709E 03	1,84601E 01
40	3,53439E 02	1,19707E 03	1,96666E 01

Note: Quoted errors are statistical only.

TABLE XVIII (Contd.)

INDEX	NEUTRØN ENERGY (KEV)	FLUX / UNIT LETHARGY	FLUX ERRØR
41	3,36608E 02	1,22371E 03	1,80841E 01
42	3,20579E 02	1,22865E 03	1,66749E 01
43	3,05314E 02	1,21259E 03	1,81343E 01
44	2,90775E 02	1,21248E 03	1,67914E 01
45	2,76928E 02	1,21176E 03	1,88451E 01
46	2,63741E 02	1,11037E 03	3,52803E 01
47	2,51182E 02	1,06312E 03	3,52766E 01
48	2,39221E 02	1,07275E 03	3,24523E 01
49	2,27830E 02	1,07023E 03	3,26742E 01
50	2,16981E 02	1,09646E 03	3,31267E 01
51	2,06648E 02	1,02787E 03	3,39723E 01
52	1,96808E 02	9,89736E 02	3,11684E 01
53	1,87436E 02	1,07909E 03	2,85902E 01
54	1,78511E 02	1,09672E 03	2,97463E 01
55	1,70010E 02	1,10669E 03	2,71325E 01
56	1,61914E 02	1,09389E 03	2,50706E 01
57	1,54204E 02	1,06872E 03	2,62783E 01
58	1,46861E 02	1,03722E 03	2,78640E 01
59	1,39868E 02	9,81900E 02	2,55576E 01
60	1,33207E 02	1,00838E 03	2,34622E 01
61	1,26864E 02	1,04158E 03	2,15929E 01
62	1,20823E 02	1,12593E 03	2,35003E 01
63	1,15069E 02	1,08322E 03	2,56826E 01
64	1,09590E 02	1,05112E 03	1,97396E 01
65	1,04371E 02	1,00494E 03	2,16241E 01
66	9,01599E 01	9,10386E 02	3,83966E 01
67	8,58666E 01	9,47877E 02	3,87022E 01
68	8,17777E 01	9,50713E 02	3,88747E 01
69	7,78835E 01	1,01873E 03	3,59083E 01
70	7,41748E 01	1,05833E 03	3,63239E 01
71	7,06427E 01	1,06729E 03	3,35995E 01
72	6,72787E 01	1,00452E 03	3,40875E 01
73	6,40750E 01	9,51859E 02	3,15827E 01
74	6,10238E 01	9,66633E 02	2,91051E 01
75	5,81179E 01	8,69205E 02	2,98701E 01
76	5,53504E 01	9,17125E 02	2,74949E 01
77	5,27146E 01	8,35426E 02	2,86562E 01
78	5,02044E 01	8,13527E 02	2,99476E 01
79	4,78137E 01	8,19414E 02	2,10887E 01
80	4,55369E 01	7,96823E 02	2,10649E 01

TABLE XVIII (Contd.)

INDEX	NEUTRØN ENERGY (KEV)	FLUX / UNIT LETHARGY	FLUX ERRØR
81	4,33685E 01	8,07219E 02	2,01070E 01
82	4,13033E 01	8,00170E 02	1,92060E 01
83	3,93365E 01	7,85361E 02	1,82389E 01
84	3,74633E 01	7,53032E 02	1,91861E 01
85	3,56793E 01	7,21411E 02	1,76818E 01
86	3,39803E 01	6,63459E 02	1,79022E 01
87	3,23622E 01	6,38578E 02	2,88723E 01
88	3,08212E 01	5,90568E 02	2,63893E 01
89	2,93535E 01	6,20417E 02	2,43541E 01
90	2,79557E 01	6,47784E 02	2,50590E 01
91	2,66245E 01	7,06870E 02	2,33701E 01
92	2,53566E 01	7,88224E 02	2,42424E 01
93	2,41492E 01	6,89923E 02	1,68470E 01
94	2,29992E 01	6,51227E 02	1,72487E 01
95	2,19040E 01	6,33850E 02	1,59785E 01
96	2,08610E 01	6,04167E 02	1,55953E 01
97	1,98676E 01	6,24930E 02	1,48804E 01
98	1,89215E 01	6,25662E 02	1,49986E 01
99	1,80205E 01	6,16136E 02	1,42095E 01
100	1,71624E 01	6,18428E 02	1,36780E 01
101	1,63451E 01	6,16728E 02	1,44622E 01
102	1,55668E 01	6,60806E 02	2,17505E 01
103	1,48255E 01	6,53322E 02	1,99581E 01
104	1,41195E 01	6,36623E 02	2,06072E 01
105	1,34472E 01	6,58516E 02	2,11452E 01
106	1,28068E 01	7,05248E 02	1,97041E 01
107	1,21970E 01	6,93605E 02	1,81283E 01
108	1,16162E 01	6,91609E 02	1,87108E 01
109	1,10630E 01	6,27414E 02	1,72848E 01
110	1,05362E 01	6,39696E 02	1,83025E 01
111	1,00345E 01	6,11915E 02	1,68244E 01
112	9,55665E 00	5,98412E 02	1,55516E 01
113	9,10158E 00	5,46816E 02	1,62247E 01
114	8,66817E 00	5,32133E 02	1,16885E 01
115	8,25540E 00	5,32018E 02	1,11656E 01
116	7,86228E 00	5,61207E 02	1,83366E 01
117	7,48789E 00	5,47257E 02	1,83298E 01
118	7,13132E 00	5,14731E 02	1,68199E 01
119	6,79174E 00	5,49447E 02	1,70838E 01
20	6,46832E 00	5,24129E 02	1,58301E 01

TABLE XVIII (Contd.)

INDEX	NEUTRØN ENERGY (KEV)	FLUX / UNIT LETHARGY	FLUX ERRØR
121	6,16030E 00	5,00173E 02	1,58419E 01
122	5,86696E 00	4,65945E 02	1,61240E 01
123	5,58758E 00	4,59021E 02	1,49915E 01
124	5,32150E 00	4,21762E 02	1,37494E 01
125	5,06810E 00	4,30021E 02	1,41274E 01
126	4,82676E 00	4,10423E 02	1,29763E 01
127	4,59691E 00	3,81287E 02	9,43642E 00
128	4,37801E 00	3,62154E 02	1,01493E 01
129	4,16954E 00	3,71794E 02	9,43125E 00
130	3,97099E 00	3,81541E 02	8,97793E 00
131	3,78189E 00	3,83644E 02	9,10922E 00
132	3,60180E 00	3,61056E 02	1,21219E 01
133	3,43029E 00	3,48293E 02	1,19638E 01
134	3,26694E 00	3,45475E 02	1,17953E 01
135	3,11137E 00	3,11645E 02	1,16761E 01
136	2,96321E 00	2,87007E 02	1,14948E 01
137	2,82211E 00	3,03182E 02	1,05881E 01
138	2,68772E 00	3,07027E 02	1,05280E 01
139	2,55973E 00	3,08209E 02	9,77138E 00
140	2,43784E 00	3,00009E 02	9,77126E 00
141	2,32175E 00	3,07235E 02	9,76472E 00
142	2,21119E 00	2,69956E 02	8,86190E 00
143	2,10590E 00	2,74573E 02	9,12985E 00
144	2,00562E 00	2,40526E 02	6,30691E 00
145	1,91011E 00	2,45647E 02	6,04688E 00
146	1,81915E 00	2,37092E 02	6,35255E 00
147	1,73253E 00	2,41770E 02	5,96122E 00
148	1,65003E 00	2,35124E 02	5,47639E 00
149	1,57145E 00	2,27376E 02	8,34701E 00
150	1,49662E 00	2,15660E 02	8,12957E 00
151	1,42536E 00	1,93944E 02	7,81339E 00
152	1,35748E 00	2,12452E 02	7,75385E 00
153	1,29284E 00	2,04584E 02	7,00422E 00
154	1,23128E 00	2,18395E 02	6,97561E 00
155	1,17264E 00	2,10076E 02	6,81412E 00
156	1,11680E 00	2,21249E 02	6,28639E 00
157	1,06362E 00	2,27368E 02	6,16784E 00
158	1,01297E 00	2,20461E 02	6,04586E 00
159	9,64737E-01	2,22955E 02	6,04817E 00
160	9,18797E-01	2,01588E 02	5,50315E 00

TABLE XVIII (Contd.)

INDEX	NEUTRØN ENERGY (KEV)	FLUX / UNIT LETHARGY	FLUX ERRØR
161	8.75045E-01	2.08930E 02	5.48255E 00
162	8.33376E-01	2.05535E 02	5.07844E 00
163	7.93691E-01	2.06490E 02	5.46934E 00
164	7.55896E-01	1.85591E 02	3.65719E 00
165	7.19901E-01	1.77463E 02	5.07148E 00
166	6.85620E-01	1.77207E 02	5.03243E 00
167	6.52972E-01	1.80297E 02	4.88118E 00
168	6.21878E-01	1.80842E 02	4.64196E 00
169	5.92265E-01	1.84271E 02	4.54748E 00
170	5.64062E-01	1.89002E 02	4.30816E 00
171	5.37201E-01	1.86193E 02	4.36668E 00
172	5.11620E-01	1.87699E 02	4.04659E 00
173	4.87258E-01	1.89437E 02	4.04724E 00
174	4.64055E-01	1.86710E 02	3.74195E 00
175	4.41957E-01	1.77848E 02	3.62651E 00
176	4.20911E-01	1.66436E 02	3.53124E 00
177	4.00868E-01	1.66546E 02	3.45373E 00
178	3.81779E-01	1.58955E 02	3.29635E 00
179	3.63599E-01	1.55323E 02	3.05329E 00
180	3.46285E-01	1.42413E 02	2.98889E 00
181	3.29795E-01	1.34207E 02	2.88676E 00

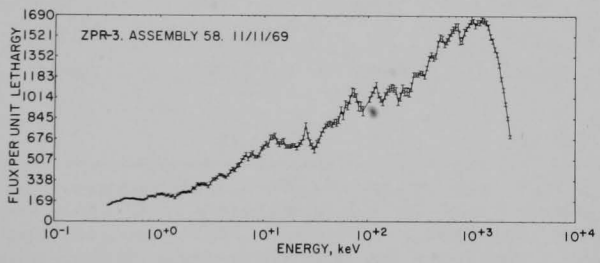

Fig. 22. Neutron Spectrum from Proton-recoil Proportional Counters. ANL Neg. No. ID-103-A2021.

8 keV has been accurately measured. Systematic errors also exist above 1 MeV, as the data-analysis model used assumes that the neutron flux goes to zero above the maximum neutron energy measured with the methane counter (2.37 MeV for this measurement). The neutron spectrum has been arranged in groups of half-lethargy widths. The resulting fluxes, given in Table XIX, are also subject to the errors discussed above.

This relatively soft neutron spectrum clearly reflects the presence of the iron in the core, especially at approximately 30 and 85 keV, which

correspond to two large iron-resonance regions. The flux depression at 750 keV may be the result of the corresponding iron resonance. Similarly, other flux depressions may be attributable to either further iron resonances or nickel, chromium, and aluminum resonances. Because of the basic overall lack of structure present in the spectrum, a true evaluation of the causes of these flux depressions is difficult.

TABLE XIX. Neutron Spectrum from Proton-recoil Proportional Counters in Half-lethargy Groups

Lower Energy, keV	Relative Flux	Lower Energy, keV	Relative Flux
1353	-	15.0	635
821	1631	9.12	647
498	1535	5.53	521
302	1317	3.35	387
183	1097	2.03	300
111	1064	1.23	225
67.4	990	0.75	212
40.9	867	0.45	184
24.8	695		

Note: For discussion of errors, see text.

APPENDIX

Safety Analysis of Assemblies 58 and 59

One safety criterion for ZPR-3 is a mandatory requirement that the calculated prompt-power coefficient in a plutonium-fueled assembly be negative. Since the design of the plutonium-aluminum fuel plates is such that the axial expansion and the associated negative temperature coefficient are small, the construction of the proposed cores 58 and 59 was contingent upon the plutonium Doppler coefficient being calculated to be zero or negative. This coefficient was calculated using the recent values of the ^{239}Pu resonance parameters. The resolved resonance parameters were taken from Schmidt.[18] Statistical parameters listed in Table A.I for the unresolved region above 300 eV were obtained from Durston and Katsuragi,[19] with the exception of $\langle\Gamma_f\rangle$ for s-wave neutrons and compound state J = 1, which was taken from Fischer.[20] The parameters in Table A.I agreed with the presently accepted ^{239}Pu alpha values.

TABLE A.I. Statistical Parameters[a] for ^{239}Pu

ℓ	0	0	1	1	1
J	0	1	0	1	2
$\langle\Gamma_n^0\rangle$, eV	0.939×10^{-3}	0.334×10^{-3}	2.195×10^{-3}	1.56×10^{-3}	0.53×10^{-3}
$\langle D\rangle$, eV	8.78	3.12	8.78	3.12	2.12
$\langle\Gamma_f\rangle$, eV	2.8	0.014-0.040	0	1.012	0.672
$\Gamma\gamma$, eV	0.0387	0.0387	0.0387	0.0387	0.0387
ν_n	1	1	1	2	1
ν_f	2	1	0	1	1

[a] ℓ = neutron angular momentum; J = compound nuclear spin; $\langle\Gamma_n^0\rangle$ = average reduced neutron width; $\langle D\rangle$ = average level spacing; $\langle\Gamma_f\rangle$ = average fission width; $\Gamma\gamma$ = radiative capture width; ν_n = number of degrees of freedom in the reduced-neutron-width chi-square distribution; and ν_f = number of degrees of freedom in the fission-width chi-square distribution.

The region compositions used in this safety analysis were similar to those in Tables I and II. Diffusion-theory calculations were performed with the MACH-1 code[6] using broad-group cross-sections at 300 and 400°K generated by the ENDF/B-MC^2 system.[21] The ^{239}Pu capture and fission cross sections in the energy range of 275 eV to 25 keV were calculated from the IDIOT code,[22] modified to include the equivalence-relation formulation from MC^2. The RABID code[23] was used to obtain the ^{239}Pu fission and capture cross sections from the resolved resonance data below 275 eV. As a check on the validity of the equivalence relation for this cell, ^{239}Pu cross sections were determined for a few small energy intervals in the region from 300 eV to 25 keV by inputting into RABID statistical resonances

generated by the RANDOM code.[24] The resonance spacings were distributed over the Wigner distribution.[18] In general, these cross sections agreed with the IDIOT-generated cross sections to within a few percent.

The temperature coefficients in the calculated critical assemblies, arising from the ^{239}Pu Doppler effect alone, were -0.93×10^{-5} and -1.40×10^{-5} $dk/k\ dT$ for the uranium- and lead-reflected systems, respectively. Both showed the required negative sign.

ACKNOWLEDGMENTS

The overall plan for the definition of the benchmark series of assemblies leading up to and including the assemblies described here was formulated by W. G. Davey and R. G. Palmer. This included specifications and review of the details of performance of these experiments. The ZPR-3 technicians performed the operation and maintenance of the reactor with enthusiasm.

REFERENCES

1. A. M. Broomfield *et al.*, *The Design and Critical Mass Determinations for ZPR-3 Assemblies 48, 48A, and 48B*, ZPR-TM-4 (1969).

2. V. C. Rogers *et al.*, "Analytical Studies of a Basic Physics Series of Plutonium Cores for ZPR-3," *Reactor Physics Division Annual Report: July 1, 1968 to June 30, 1969*, ANL-7610 (Jan 1970).

3. C. F. Masters, M. M. Thorpe, and D. B. Smith, *Measurement of Absolute Delayed Neutron Yields from 14 MeV Fission*, Trans. Am. Nucl. Soc. *11*, 179 (1968).

4. S. G. Carpenter and S. Ramchandran, β_{eff} *Ratio Measurements*, Trans. Am. Nucl. Soc. *12*, 650 (1969).

5. R. G. Matlock, R. E. Kaiser, and J. M. Gasidlo, *Reactivity Effects in Critical Facilities due to Fissile Isotope Decay*, Trans. Am. Nucl. Soc. *12*, 652 (1969).

6. D. A. Meneley, L. C. Kvitek, and D. M. O'Shea, *MACH-1, A One-dimensional Diffusion-theory Package*, ANL-7223 (June 1966).

7. G. R. Keepin, *Neutron Data for Reactor Kinetics*, Nucleonics *20*, 8, 150 (1962).

8. E. F. Bennett and R. L. Long, *Precision Limitations in the Measurements of Small Reactivity Changes*, Nucl. Sci. Eng. *17*, 425 (1963).

9. S. G. Carpenter, J. M. Gasidlo, and J. M. Stevenson, β_{eff} *Measurements in Two Fast Reactor Critical Assemblies*, Trans. Am. Nucl. Soc. *13*, 92 (1970).

10. F. S. Kirn, "Neutron Detection with an Absolute Fission Counter," *Proceedings of a Symposium on Neutron Detection, Dosimetry and Standardization*, Vol. II, p. 497, IAEA (1963).

11. W. G. Davey and P. I. Amundson, *Inelastic Scattering Measurements in a Fast Reactor by the Spherical Shell Method*, Nucl. Sci. Eng. *28*, 111 (1967).

12. A. L. Hess, Q. L. Baird, and A. M. Broomfield, *Material Worth Measurements in ZPR-3 Assemblies 48, 48A, and 48B*, ZPR-TM-7 (1969).

13. J. M. Gasidlo *et al.*, *Doppler Effect, Heterogeneity, and Sodium Voiding Experiments in ZPR-3 Assemblies 48 and 48B*, ZPR-TM-8 (1969).

14. T. J. Yule and E. F. Bennett, "Use of a Small Computer for Proton-recoil Proportional Counting," *Reactor Physics Division Annual Report: July 1, 1967 to June 30, 1968*, ANL 7410, pp. 358-360 (Jan 1969).

15. E. F. Bennett, *Fast Neutron Spectroscopy by Proton-recoil Proportional Counting*, Nucl. Sci. Eng. *27*, 16 (1967).

16. J. E. Powell and J. M. Larson, Argonne National Laboratory, private communication (1969).

17. E. F. Bennett, R. Gold, and I. K. Olson, *Analysis and Reduction of Proton-recoil Data*, ANL-7394 (Jan 1968).

18. J. J. Schmidt, *Neutron Cross Sections for Fast Reactor Materials*, KFK-120 (1966).

19. C. Durston and S. Katsuragi, *On the Evaluation of Pu-239 Data in the keV and Resolved Resonance Region*, JAERI-1162 (1968).

20. E. A. Fischer, *Interpretation von Dopplerprobenmessungen in Schnellen Kritischen Null-Energie-Anlagen*, KFK-844 (1969).

21. B. J. Toppel, A. L. Rago, and D. M. O'Shea, *MC^2, A Code to Calculate Multigroup Cross Sections*, ANL-7318 (June 1967).

22. T. A. Pitterle and D. M. Green, APDA, unpublished (1966).

23. A. P. Olson, *RABID: An Integral Transport-theory Code for Neutron Slowing Down in Slab Cells*, ANL-7645 (Apr 1970).

24. G. L. Grasseschi and V. C. Rogers, Argonne National Laboratory, private communication (1969).

ARGONNE NATIONAL LAB WEST
3 4444 00008289 1
ARGONNE NATIONAL LAB WEST
3 4444 00008289 1
ARGONNE NATIONAL LAB WEST
3 4444 00008289 1
ARGONNE NATIONAL LAB WEST
3 4444 00008289 1
ARGONNE NATIONAL LAB WEST
3 4444 00008289 1
ARGONNE NATIONAL LAB WEST
3 4444 00008289 1
ARGONNE NATIONAL LAB WEST
3 4444 00008289 1
ARGONNE NATIONAL LAB WEST
3 4444 00008289 1
ARGONNE NATIONAL LAB WEST
3 4444 00008289 1
ARGONNE NATIONAL LAB WEST
3 4444 00008289 1